PHYSICAL REVIEW E VOLUME 57, NUMBER 5 MAY 1998

Measurement of the stimulated Brillouin scattering reflectivity from a spatially smoothed laser beam in a homogeneous large scale plasma

S. D. Baton, F. Amiranoff, V. Malka, A. Modena, M. Salvati, and C. Coulaud
LULI, CNRS, Ecole Polytechnique, 91128 Palaiseau Cedex, France

C. Rousseaux and N. Renard
CEA Limeil-Valenton, 94195 Villeneuve-St.-Georges Cedex, France

Ph. Mounaix
CPhT, CNRS, Ecole Polytechnique, 91128 Palaiseau Cedex, France

C. Stenz
Grémi, Université d'Orléans, 45067 Orléans Cedex 2, France

(Received 27 October 1997)

The dependence of the stimulated Brillouin scattering (SBS) reflectivity on both the focusing aperture and the incident laser intensity has been experimentally studied in the case of a spatially smoothed beam. The experiment was performed in millimeter size, homogeneous, stationary plasmas created by irradiating a helium gas jet. SBS was excited by a 1.053-μm wavelength, 600-ps interaction beam at intensities up to 4×10^{14} W/cm^2. The saturation level of SBS reflectivities was of the order of 10%. A good agreement between the experimental SBS thresholds and the theoretical ones obtained from the one-dimensional stochastic convective SBS model [Phys. Plasmas **2**, 1804 (1995)] is observed. [S1063-651X(98)50205-X]

PACS number(s): 52.40.Nk, 52.35.Mw, 42.65.Es

Although extensively studied for many years, both theoretically [1] and experimentally [2] the stimulated Brillouin scattering (SBS) instability is still poorly understood. SBS is a parametric instability in which an incident light wave resonantly decays into a scattered light wave and an ion acoustic wave [3] This instability can grow over a large volume of plasma, whenever the inequality $n_e/n_c<1$ is satisfied; here n_e and n_c denote the electron and critical density, respectively. Since SBS has a great potential for scattering (typically in the backward direction) and redistributing the incident light energy, it is an important issue for inertial confinement fusion (ICF), both in direct and indirect drive schemes [4]. The work reported here presents measurements of SBS reflectivity from millimeter-size plasmas of interest to ICF. The interaction beam was spatially smoothed, using the random-phase plate (RPP) smoothing technique [5]. It was focused into the preformed plasma with two different F numbers where F refers to the focusing aperture. In these experimental conditions, the onset of the SBS reflectivity is expected at some threshold intensity essentially due to the statistical intensity distribution produced in the focal volume by the RPP [6]. In previous experiments performed in homogeneous plasmas by Watt *et al.* [7] (exploding foil plasma) and by Fernandez *et al.* [8] (large *hohlraum* plasma), a qualitative agreement between the experimental and the calculated F dependence of the threshold intensity was found. In inhomogeneous plasmas, a quantitative agreement was observed by Drake *et al.* [9]. In the reported experiment, performed in homogeneous and stationary plasmas, the measurements are shown to agree quantitatively with the theory.

The experiment was performed using the multibeam laser facility at The Laboratoire pour l'Utilisation des Lasers Intenses (LULI). The pulse duration of the Gaussian beams was 600 ps full width at half maximum (FWHM). The creation beam used to preform the plasma was operated at twice the fundamental frequency of the Nd-glass laser (0.53 μm). It was focused with an $F=6$ aperture lens at the center of a cylindrical supersonic helium gas jet of 2.5-mm diameter. The gas was fully ionized by collisional ionization along the whole length of the jet perpendicular to the gas flow. This beam was spatially smoothed by a 2-mm cell size RPP. The diameter of the focal spot corresponding to the first Airy zero was 320 μm, yielding a spatially averaged intensity of 4×10^{13} W/cm^2.

The interaction beam, at the fundamental frequency (1.053 μm), was fired in the opposite direction of the creation beam after a time delay of 1 ns (the delay is the time separating the maxima of the pulses). This beam was spatially smoothed by using a 4-mm cell RPP with two focusing lenses: 500-mm focal length ($F=6$) and 250-mm focal length ($F=3$). The energy of the interaction beam was varied from 60 mJ to 60 J by locating neutral optical-quality attenuators in the beam. In the following, the mean experimental intensity is defined by taking the ratio of 80% of the incident energy to the product of the pulse duration (600 ps) by the Airy focal spot area (first Airy zero radius). This gave maximum intensities of 10^{14} and 4×10^{14} W/cm^2 for $F=6$ and $F=3$, respectively. The focal spot images, obtained in transmission in vacuum, were in agreement with the calculated ones.

The backscattered light was collected through the focusing lens ($F=3$ or $F=6$) and analyzed by two photodiodes. The first one (fast S1 photodiode) associated with a 7-GHz scope measured the SBS energy. The second one measured the stimulated-Raman-scattering (SRS) energy; we used a fast InGaAs photodiode (300-ps rise time) characterized by a

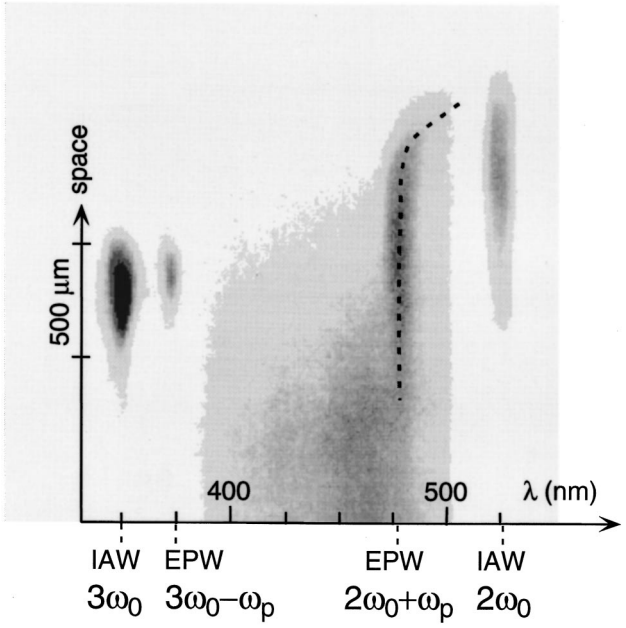

FIG. 1. Space-resolved Thomson scattering spectrum. The interaction beam comes from the bottom of the figure. On the right is the Thomson self-scattering of the creation beam; the dashed line represents the jet density profile. On the left is the Thomson scattering on the SBS-driven IAW and on the SRS-driven EPW. The low contrast between the background emission and the Thomson self-scattering is due to the plasma noise emission integrated over several nanoseconds (because of the low sweep speed of the streak camera).

nearly constant sensitivity in the range of 1.1-–1.6-μm wavelength. Simultaneously, the SRS light was spectrally analyzed with the help of an InGaAs detector array associated with a spectrometer. Each photodiode was adequately filtered to suppress the undesirable wavelengths. In addition, the transmitted energy and the image of the interaction beam focal spot were recorded systematically.

A third beam was used as a Thomson scattering diagnostic to probe the electron plasma wave (EPW) and ion acoustic wave (IAW) driven by the interaction beam. This probe beam, frequency tripled (0.35 μm), was fired 200 ps before the interaction beam and line-focused along the direction of the interaction beam. The scattered light from the probe beam was collected at 100° from the laser axis by an $F=3$ spherical mirror. A high (low) spectral-dispersion spectrometer coupled to a streak camera was used to analyze the IAW (EPW). An optical device allowed us to rotate the image of the plasma by 90° along the slit of the low-dispersion imaging spectrometer. Thus we could choose to analyze the spectrum either with time resolution or with spatial resolution (along the propagation axis of the interaction beam). The spatially resolved spectrum was obtained both by setting a low sweep speed on the streak camera and by removing its entrance slit. Because of the low spectral dispersion, we then obtained, on the same record and along the laser axis, components coming from the interaction beam and from the creation beam.

Figure 1 shows a typical spatially resolved spectrum. The creation beam comes from the top and the interaction beam from the bottom. From left to right, the first two signals

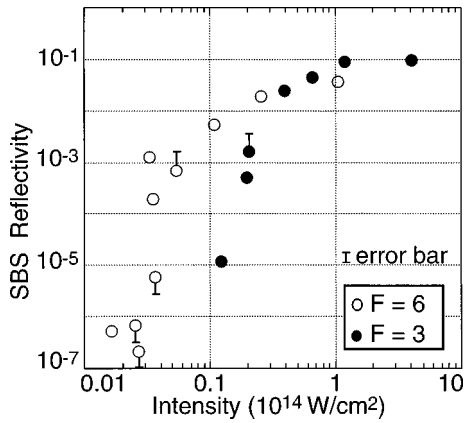

FIG. 2. Experimental SBS reflectivities as a function of the laser intensity for the two F numbers ($F=3$ and 6).

correspond to the Thomson scattering on the IAW ($3\omega_0$) and EPW ($3\omega_0-\omega_p$) driven by SBS and SRS, respectively. Here ω_0 denotes the fundamental laser frequency and ω_p the plasma frequency. The study of the location of these waves and their relative intensities is beyond the scope of this paper and will be the subject of a following one. The next two signals come from the thermal Thomson self-scattering of the creation beam on the EPW ($2\omega_0+\omega_p$) and IAW ($2\omega_0$). The scattered signal on the EPW of the creation beam allows us to infer the spatial profile of the electron density along the interaction axis. Typically, with a backing pressure of 60 bars, the plasma is quasihomogeneous over 2 mm with an electron density around 2 to 2.5×10^{19} cm^{-3}. This density is inferred either from the scattering on the thermal EPW or from the backward SRS spectra. The electron temperature deduced from IAW time-resolved spectra (not shown here) is found to be 250–300 eV. The ion temperature is estimated to around 60–70 eV by using numerical fit of the time-resolved spectra of IAW. The transmission rate ranged between 25% and 40%.

Measurements of backward SRS always showed reflectivities below 10^{-3}. Such a low SRS reflectivity may be due to the Landau damping of the SRS-EPW; at 300 eV and 2.2% of n_c, the value of $k\lambda_D$ is 0.3, corresponding to strong Landau damping (k and λ_D denote the EPW wave number and the Debye length, respectively). It is therefore reasonable to consider that in this experiment SRS does not affect SBS significantly.

Figure 2 shows the SBS reflectivity as a function of the laser intensity for two F numbers. Here the reflectivity is defined as the ratio of the SBS energy backscattered through the focusing lens to the incident laser energy. Two remarkable features can be observed: (i) the SBS reflectivity saturates at the same level (from a few percent to 10%) without any significant dependence on the focusing conditions. It is also interesting to mention that the IAW spectra are very similar for the two interaction conditions; (ii) the SBS reflectivity sharply increases at a threshold laser intensity, which strongly depends on the F number. This threshold is about $(2-2.5)\times10^{13}$ W/cm^2 for $F=3$ and $(4-5)\times10^{12}$ W/cm^2 for $F=6$. In the following, we focus on the interpretation of point (ii).

In this paragraph, we elaborate on some technical points of our computation of the theoretical SBS threshold deter-

mined as the average laser intensity at which the linear amplification factor diverges. We have compared the experimental values of the SBS threshold to the theoretical ones obtained from the one-dimensional (1D) stochastic convective amplifier model of Ref. [10] (cf., remark [11]). In this model, the backscattered SBS intensity is computed in terms of the correlation function of the 1D pump field $C(x)$. A realistic expression for $C(x)$ can be obtained from the on-axis correlation function of an actual three-dimensional (3D) ''top-hat'' RPP field. Namely [12],

$$C(x)=\exp(-1.39ix/\Lambda_{\parallel})\,\frac{\sin(1.39x/\Lambda_{\parallel})}{1.39x/\Lambda_{\parallel}}, \qquad (1)$$

where $\Lambda_{\parallel}$ is the hot spot length, defined as the half width at half maximum of $|C(x)|^2$: $\Lambda_{\parallel}\approx 0.885(1+4F^2)\lambda_0$. Unfortunately, it can be shown [10] that the SBS threshold for a finite SBS active region length L can be computed analytically only if the correlation function of the RPP field $C(x)$ is of the exponential form $C(x)=\exp(-|x|/l_c)$, where l_c is the correlation length. The problem is thus to find a relation between l_c and $\Lambda_{\parallel}$ in order for the exponential model to be in a good quantitative agreement with the more realistic one corresponding to Eq. (1). Since in the limit $L\leqslant\Lambda_{\parallel}$ the threshold is expected not to be very sensitive to the speckle shape, we have chosen l_c so that the thresholds of the two models coincide in the opposite limit $L\gg\Lambda_{\parallel}$. Note that this procedure significantly improves the previous ones proposed in Ref. [10] (second reference). From Eq. (6) of Ref. [10] the SBS threshold in the limit of a large $L/\Lambda_{\parallel}$ is given by

$$\lim_{n\to+\infty}\frac{4\pi}{l_G}\left[\int_{-\infty}^{+\infty}C(k)^{n+1}dk\right]\Big/\left[\int_{-\infty}^{+\infty}C(k)^{n}dk\right]=1, \qquad (2)$$

where l_G is the average SBS convective amplification length for the amplitude and $C(k)$ is the Fourier transform of $C(x)$ defined by $C(k)=(1/2\pi)\int C(x)\exp(-ikx)dx$. For $C(x)$ given by Eq. (1), one has $C(k)=(\Lambda_{\parallel}/2.78)H[-k(k+2.78/\Lambda_{\parallel})]$, where H is the Heaviside step function, and Eq. (2) gives the threshold $\Lambda_{\parallel}/l_G=(2.78/4\pi)$. In the same limit the exponential model yields $l_c/l_G=0.25$. Equating the two thresholds, one obtains $\Lambda_{\parallel}=0.885l_c$. Inserting then this relation into Eq. (10) of Ref. [10], one finds the following analytical expression linking the SBS active region length L (normalized to the hot spot length $\Lambda_{\parallel}$) and the average hot spot convective gain at threshold $G_{\rm hot}\equiv 2\Lambda_{\parallel}/l_G$:

$$\frac{L}{\Lambda_{\parallel}}=\frac{1.13}{\sqrt{2.26G_{\rm hot}-1}}\tan^{-1}\left[\frac{\sqrt{2.26G_{\rm hot}-1}}{1.13G_{\rm hot}-1}\right], \qquad (3)$$

where the determination of $\tan^{-1}$ is such that $0<\tan^{-1}\leqslant\pi$. In physical units, $G_{\rm hot}$ reads

$$G_{\rm hot}\approx\frac{2.6\times10^{-2}\tilde{n}_e\langle I_{14}\lambda^2\rangle(1+4F^2)}{T_e[1+3\Delta_{\rm IAW}T_i/ZT_e]\Delta_{\rm IAW}\tilde{\nu}_{\rm IAW}\sqrt{1-\tilde{n}_e}}, \qquad (4)$$

where $\langle I_{14}\lambda^2\rangle=3.26I_{14}\lambda^2$ is the average laser flux at threshold in units of 10^{14} W cm^{-2} μm^2, corresponding to the highest intensity FWHM region of the focal spot in which most of the SBS is generated ($I_{14}\lambda^2$ denoting the experimental spatially averaged intensity in the first Airy zero) [13]. In Eq. (4), T_e and T_i are the electron and ion temperatures in units of keV, $\tilde{n}_e=n_e/n_c$, $\tilde{\nu}_{\rm IAW}=\nu_{\rm IAW}/\omega_{\rm IAW}$ is the damping of the SBS-driven ion acoustic wave normalized to its angular frequency, and the quantity $\Delta_{\rm IAW}$ is given by $\Delta_{\rm IAW}\equiv 1+k_{\rm IAW}^2\lambda_D^2$ where $k_{\rm IAW}^2\lambda_D^2=7.83\times10^{-3}T_e(\tilde{n}_e^{-1}-1)$. To take into account both Landau and collisional effects we have computed the normalized damping $\tilde{\nu}_{\rm IAW}$ from the empirical expressions of Ref. [14]. Equations (3) and (4) can be solved to find relations among chosen parameters at threshold.

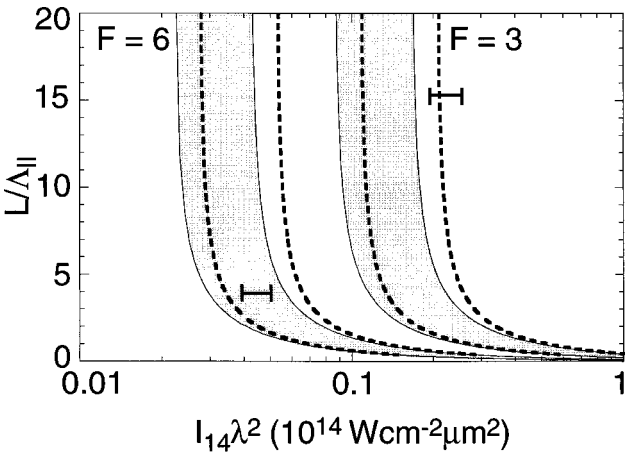

FIG. 3. Experimental and theoretical SBS thresholds in the plan $(L/\Lambda_{\parallel},I_{14}\lambda^2)$ for the two F numbers ($F=3$ and 6). $L\approx500$ μm is the length of the SBS active region, and $\Lambda_{\parallel}$ is the hot spot length ($L/\Lambda_{\parallel}=15.3$ for $F=3$ and $L/\Lambda_{\parallel}=3.9$ for $F=6$). The horizontal bars are the experimental results [$(2-2.5)\times10^{13}$ W/cm^2 for $F=3$ and $(4-5)\times10^{12}$ W/cm^2 for $F=6$]. The shaded regions correspond to the 1D theoretical thresholds over the estimated range of the experimental plasma parameters: $2\%\leqslant n_e/n_c\leqslant2.5\%$, $250\leqslant T_e$ (eV)$\leqslant300$, and $60\leqslant T_i$ (eV)$\leqslant70$. The dashed lines represent the theoretical thresholds modified to take into account the 3D effects heuristically.

Figure 3 shows the experimental and theoretical SBS thresholds, in the plan $(L/\Lambda_{\parallel},I_{14}\lambda^2)$, for the two F numbers $F=3$ and 6. According to the Thomson scattering spectra, the length of the SBS active region at threshold L is the same in the two cases, namely $L\approx500$ μm. The horizontal bars represent the experimental results. The shaded regions correspond to the 1D theoretical thresholds from Eqs. (3) and (4) over the estimated range of the experimental plasma parameters [$2\%\leqslant n_e/n_c\leqslant2.5\%$, $250\leqslant T_e$ (eV)$\leqslant300$, and $60\leqslant T_i$ (eV)$\leqslant70$]. It can be seen that for $F=6$ there is a very good agreement between the experimental and theoretical thresholds. On the other hand, for $F=3$ the theoretical threshold is about half the actual one. This discrepancy can be partly attributed to 3D effects, which tend to increase the threshold in the large L limit as compared to a simple 1D calculation [10]. To take into account such 3D effects heuristically, we have adjusted the relation between l_c and $\Lambda_{\parallel}$ so that the critical curve for the average amplitude given by the 1D model of Ref. [10] fits the 3D numerical results in Fig. 2 of Ref. [6] as well as possible. We have obtained the relation $\Lambda_{\parallel}=1.107l_c$ that we have inserted into Eq. (10) of Ref. [10]. This procedure should yield a SBS threshold fairly close to the actual 3D one. The result is displayed in Fig. 3 (dashed lines).

The agreement between the experimental and theoretical results one obtains is better than in previous experiments performed with RPP beams by Watt *et al.* [7] and Fernandez *et al.* [8], where only a qualitative agreement was observed. This difference can be partly attributed to different definitions of the quantity $\langle I_{14}\lambda^2\rangle$. For instance, Watt *et al.* have used $\langle I_{14}\lambda^2\rangle=(I_{14}\lambda^2)_{\max}$, where $(I_{14}\lambda^2)_{\max}$ is the peak intensity of one RPP element diffraction pattern. Since this definition corresponds to the largest possible value of $\langle I_{14}\lambda^2\rangle$, one can reasonably expect that it overestimates the contribution of the highest intensity region of the focal spot. If they had used the same definition as ours, they would have found a better quantitative agreement with the theory. On the other hand, a possible explanation put forward by these authors for that poor quantitative agreement was that their experimental conditions were incompatible with the ideal plasma conditions required for the models of Refs. [6] or [10], i.e., homogeneous plasma, no hot spot self-focusing, and (for the former experiment) an important level of SRS interacting with SBS, thus affecting its threshold. In our case, the experimental conditions were much closer to the ones required by the models: (i) using a gas jet made it possible to obtain a very good plasma homogeneity; (ii) the low density of the plasma prevented self-focusing from enhancing SBS. Indeed, at low density the critical power for the onset of self-focusing increases and the inhibiting effect of density depletion on SBS in a self-focused hot spot dominates the intensity enhancement effect [15]. Note that since this inhibiting effect is expected to be more effective for small F numbers, it might be a possible explanation for the slight remaining underestimation of the $F=3$ experimental threshold, which can be seen in Fig. 3; (iii) finally, as previously mentioned, we never measured SRS reflectivities above 10^{-3} and we can consider that SRS does not affect SBS significantly in this experiment.

In conclusion, we have performed measurements of SBS reflectivity from a spatially smoothed laser beam in a homogeneous large-scale gas-jet plasma. We have studied the dependence of the SBS reflectivity on both the focusing aperture and the incident laser intensity. The experimental SBS thresholds are found to be in good quantitative agreement with theoretical ones. This agreement can be attributed to our experimental conditions, which were close to the ideal ones required by the models.

[1] J. F. Drake *et al.*, Phys. Fluids **17**, 778 (1974); C. S. Liu, M. N. Rosenbluth, and R. B. White, *ibid.* **17**, 1211 (1974); D. W. Forslund, J. M. Kindel, and E. L. Lindman, *ibid.* **18**, 1002 (1975).

[2] H. A. Baldis, E. M. Campbell, and W. L. Kruer, in *Handbook of Plasma Physics,* edited by A. Rubenchik and S. Witkowski (North-Holland, Amsterdam, 1992), Vol. 3, and references therein.

[3] W. L. Kruer, *The Physics of Laser Plasma Interactions* (Addison-Wesley, New York, 1988).

[4] J. Lindl, Phys. Plasmas **2**, 3933 (1995).

[5] Y. Kato *et al.*, Phys. Rev. Lett. **53**, 1057 (1984).

[6] H. A. Rose and D. F. DuBois, Phys. Rev. Lett. **72**, 2883 (1994).

[7] R. G. Watt *et al.*, Phys. Plasmas **3**, 1091 (1996).

[8] J. C. Fernandez *et al.*, Phys. Rev. E **53**, 2747 (1996).

[9] R. P. Drake, R. G. Watt, and K. Estabrook, Phys. Rev. Lett. **77**, 79 (1996).

[10] Ph. Mounaix, Phys. Plasmas **2**, 1804 (1995); **3**, 3867 (1996).

[11] We have not used the 3D numerical results displayed in Fig. 2 of Ref. [6] since (i) these results concern the threshold for the amplitude (not the intensity) and (ii) the considered range of interaction lengths is not large enough for our experimental conditions.

[12] H. A. Rose and D. F. DuBois, Phys. Fluids B **5**, 590 (1993).

[13] This definition of $\langle I_{14}\lambda^2\rangle$ is a reasonable compromise between $\langle I_{14}\lambda^2\rangle=I_{14}\lambda^2$, which clearly underestimates the contribution of the high-intensity region of the focal spot, and the opposite limit $\langle I_{14}\lambda^2\rangle=(I_{14}\lambda^2)_{\max}$ (taken by Watt *et al.* in Ref. [7]), where $(I_{14}\lambda^2)_{\max}$ is the peak intensity of one RPP element diffraction pattern, which, on the contrary, overestimates this contribution.

[14] M. Casanova, Laser Part. Beams **7**, 165 (1989).

[15] V. T. Tikhonchuk, S. Hüller, and Ph. Mounaix, Phys. Plasmas **4**, 4369 (1997).